

Relation of V/III ratio of AlN interlayer with the polarity of nitride

Zhaole Su(苏兆乐), Yangfeng Li(李阳锋), Xiaotao Hu(胡小涛), Yimeng Song(宋祎萌), Zhen Deng(邓震), Ziguang Ma(马紫光), Chunhua Du(杜春花), Wenxin Wang(王文新), Haiqiang Jia(贾海强), Yang Jiang(江洋), and Hong Chen(陈弘)

Citation: Chin. Phys. B, 2024, 33 (**11**): 117801. DOI: 10.1088/1674-1056/ad71b2
Journal homepage: http://cpb.iphy.ac.cn; http://iopscience.iop.org/cpb

What follows is a list of articles you may be interested in

Investigation of reflection anisotropy induced by micropipe defects on the surface of a 4H-SiC single crystal using scanning anisotropy microscopy

Wei Huang(黄威), Jinling Yu(俞金玲), Yu Liu(刘雨), Yan Peng(彭燕),Lijun Wang(王利军), Ping Liang(梁平), Tangsheng Chen(陈堂胜), Xiangang Xu(徐现刚), Fengqi Liu(刘峰奇), and Yonghai Chen(陈涌海)
Chin. Phys. B, 2024, 33 (**3**): 037801. DOI: 10.1088/1674-1056/acf27f

Crystal and electronic structure of a quasi-two-dimensional semiconductor $Mg_3Si_2Te_6$

Chaoxin Huang(黄潮欣), Benyuan Cheng(程本源), Yunwei Zhang(张云蔚), Long Jiang(姜隆), Lisi Li(李历斯), Mengwu Huo(霍梦五), Hui Liu(刘晖), Xing Huang(黄星), Feixiang Liang(梁飞翔), Lan Chen(陈岚), Hualei Sun(孙华蕾), and Meng Wang(王猛)
Chin. Phys. B, 2023, 32 (**3**): 037802. DOI: 10.1088/1674-1056/aca393

Magnetic polaron-related optical properties in Ni(II)-doped CdS nanobelts: Implication for spin nanophotonic devices

Fu-Jian Ge(葛付建), Hui Peng(彭辉), Ye Tian(田野), Xiao-Yue Fan(范晓跃), Shuai Zhang(张帅), Xian-Xin Wu(吴宪欣), Xin-Feng Liu(刘新风), and Bing-Suo Zou(邹炳锁)
Chin. Phys. B, 2022, 31 (**1**): 017802. DOI: 10.1088/1674-1056/ac0782

Efficiency droop in InGaN/GaN-based LEDs with a gradually varying In composition in each InGaN well layer

Shang-Da Qu(屈尚达), Ming-Sheng Xu(徐明升), Cheng-Xin Wang(王成新), Kai-Ju Shi(时凯居), Rui Li(李睿), Ye-Hui Wei(魏烨辉), Xian-Gang Xu(徐现刚), and Zi-Wu Ji(冀子武)
Chin. Phys. B, 2022, 31 (**1**): 017801. DOI: 10.1088/1674-1056/ac0817

Signal-to-noise ratio of Raman signal measured by multichannel detectors

Xue-Lu Liu(刘雪璐), Yu-Chen Leng(冷宇辰), Miao-Ling Lin(林妙玲), Xin Cong(从鑫), and Ping-Heng Tan(谭平恒)
Chin. Phys. B, 2021, 30 (**9**): 097807. DOI: 10.1088/1674-1056/ac1f06

Relation of V/III ratio of AlN interlayer with the polarity of nitride

Zhaole Su(苏兆乐)[1,2], Yangfeng Li(李阳锋)[1,2], Xiaotao Hu(胡小涛)[1,2], Yimeng Song(宋祎萌)[4], Zhen Deng(邓震)[1,2,5], Ziguang Ma(马紫光)[1,2], Chunhua Du(杜春花)[1,2], Wenxin Wang(王文新)[1,2], Haiqiang Jia(贾海强)[1,2,3], Yang Jiang(江洋)[1,2,†], and Hong Chen(陈弘)[1,2,3,‡]

[1] *Key Laboratory for Renewable Energy, Beijing Key Laboratory for New Energy Materials and Devices, Beijing National Laboratory for Condensed Matter Physics, Institute of Physics, Chinese Academy of Sciences, Beijing* 100190, *China*
[2] *University of Chinese Academy of Sciences, Beijing* 100049, *China*
[3] *Songshan Lake Materials Laboratory, Dongguan* 523808, *China*
[4] *School of Mathematics and Physics, Beijing Key Laboratory for Magneto-Photoelectrical Composite and Interface Science, University of Science and Technology Beijing, Beijing* 100083, *China*
[5] *The Yangtze River Delta Physics Research Center, Liyang* 213000, *China*

(Received 21 December 2023; revised manuscript received 27 June 2024; accepted manuscript online 21 August 2024)

N-polar GaN film was obtained by using a high-temperature AlN buffer layer. It was found that the polarity could be inverted by a thin low-temperature AlN interlayer with the same V/III ratio as that of the high-temperature AlN layer. Continuing to increase the V/III ratio of the low-temperature AlN interlayer, the Ga-polarity of GaN film was inverted to N-polarity again but the crystal quality and surface roughness of GaN film greatly deteriorated. Finally, we analyzed the chemical environment of the AlN layer by x-ray photoelectron spectroscopy (XPS), which provides a new direction for the control of GaN polarity.

Keywords: semiconductors, III–V semiconductors, chemistry of MOCVD and other vapor deposition methods

PACS: 78.55.Cr, 61.82.Fk, 71.55.Eq, 82.33.Ya **DOI:** 10.1088/1674-1056/ad71b2

1. Introduction

Gallium nitride (GaN) and related materials are very promising with broader application prospects in the areas of ultraviolet and deep ultraviolet detectors, high electron mobility transistors, blue-green light emitting diodes, and so on.[1] The polarity of GaN films includes Ga polarity, N polarity, non-polarity and semi-polarity. The most commonly and widely used Ga-polar GaN is the easiest to grow and the crystal quality is the best. N-polar GaN is attracting more attention because of its multiple potentials in reducing efficiency droop and threshold current density of laser diodes,[2] enhancing the incorporation of indium into InGaN multiple quantum wells.[3] The polarity control of GaN films is a very important problem. N-polar GaN template can be initially inverted to Ga polarity by a 10 nm LT AlN interlayer,[4] AlN/AlO_x interlayer,[5] or trimethylaluminum preflow in MOCVD.[6] Stolyarchuk *et al.* also intentionally inverted the polarity of N-polar AlN film by oxygen treatment.[7] We realized the growth of high-quality N-polar GaN films on sapphire substrate by a high temperature (HT) AlN buffer layer with high V/III (>10000) ratio,[8] and then found that a thin low temperature (LT) AlN interlayer can achieve polarity inversion, but a low temperature GaN interlayer cannot.[9] However, the polarity inversion mechanism of the LT AlN layer is not clear. In this paper, we found that the V/III ratio of LT AlN interlayer is pivotal for the control of polarity, and explored the effect of LT AlN interlayer with different V/III ratios on the quality of subsequent GaN film in detail.

2. Experiment

GaN films were grown on vicinal sapphire substrates with a misorientation angle of 2° toward M axis (labeled as 2M) using an Aixtron close-coupled showerhead MOCVD system. Trimethylgallium (TMGa), trimethylaluminum (TMAl) were used as group III sources and ammonia (NH_3) was used as group V source, hydrogen was used as carrier gas. The sapphire substrates were baked 7 min under H_2 atmosphere to wipe off impurities on the surface. HT AlN with a thickness of 100 nm was grown at the temperature of 1050 °C. The flow rates of TMAl and NH_3 source were 136 sccm and 12000 sccm, respectively. Then, for sample A, a 1.5 μm HT GaN layer was grown directly on the AlN buffer layer at a temperature of 1020 °C. For samples B and C, a thin LT AlN interlayer (about 10 nm) with different V/III ratio was grown at a temperature of 700 °C just after the growth of HT AlN layer. Finally, a 1.5 μm GaN layer was grown with the same condition as sample A. Schematic diagrams of samples A-C are shown in Fig. 1 and the growth condition of the LT AlN interlayer is shown in Table 1.

†Corresponding author. E-mail: jiangyang@iphy.ac.cn
‡Corresponding author. E-mail: hchen@iphy.ac.cn

© 2024 Chinese Physical Society and IOP Publishing Ltd

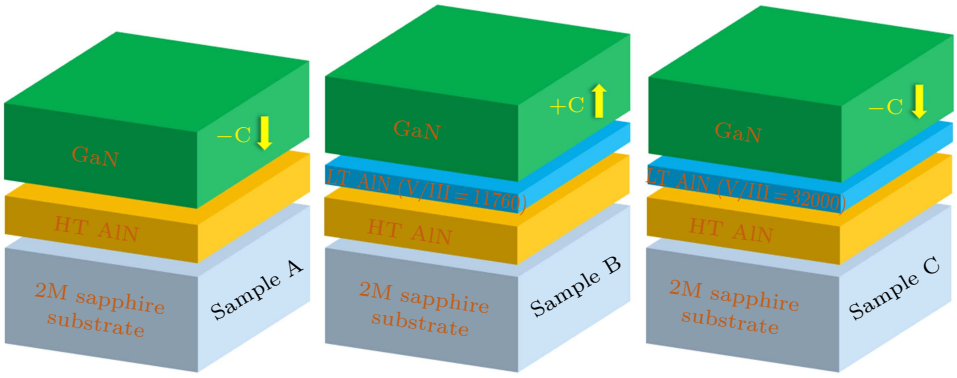


Fig. 1. Schematic diagrams of samples A–C.

Table 1. The source flow rates of LT AlN interlayer.

Sample	TMAl	NH_3	V/III ratio
A	*	*	*
B	136	12000	11760
C	100	24000	32000

The growth process was monitored by *in situ* reflectance spectrum, the surface morphology of these samples was characterized by scanning electron microscopy (SEM) and atomic force microscopy (AFM). The crystal quality of the GaN layers was measured by HRXRD. To get the mechanism of polarity inversion, the growth process was interrupted after the AlN layer and these three interrupted samples were studied by x-ray photoelectron spectroscopy (XPS) and AFM.

3. Results and discussion

To monitor the growth process of nitrides in real time, an *in situ* reflectance spectrum was carried out and the result is shown in Fig. 2. The wavelength of the laser was 633 nm and the direction of laser light was perpendicular to the surface of the wafer. For samples A and B, the reflectance oscillated directly at the beginning of GaN layer growth, indicating a two-dimensional growth mode. However, the amplitude of sample B decreased dramatically, implying a rougher surface morphology. It was interesting that the reflectance of sample C decreased abruptly to about zero and then increased gradually. This was a common phenomenon of roughening-recovery process in the growth of Ga-polar GaN materials.

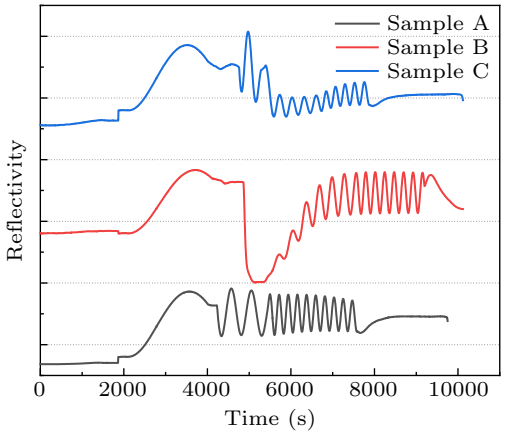


Fig. 2. *In situ* reflectance spectrums of samples A–C.

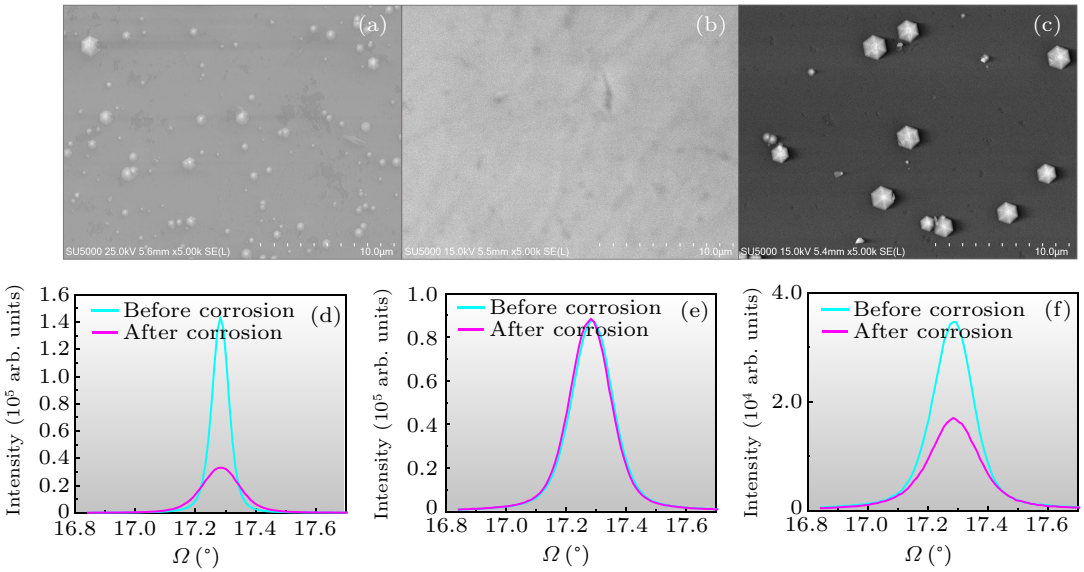


Fig. 3. (a)–(c) SEM images of samples A–C after hot KOH solution corrosion and (d)–(f) (002) x-ray rocking curve comparison before and after corrosion.

To verify the polarity, these samples were put into hot (80 °C) KOH (1 mol/L) solution for 10 min. It is well known that N-polar GaN film can be corroded easily by OH^- but Ga-polar GaN film cannot.[10] The corrosion results are shown in Fig. 3. There were several hexagonal pyramids on the surface of samples A and C after corrosion. However, the surface of sample B was still smooth. The (002) x-ray rocking curves were measured before and after KOH solution corrosion, respectively. After corrosion, the intensity of rocking curve of samples A and C declined evidently. However, for sample B, the XRD intensity remained unchanged. This result implies that samples A and C were mostly corroded off but sample B remained stable. Thus, samples A and C were N-polar and sample B was Ga-polar.

To evaluate the crystal quality, HRXRD was carried out and the (002)/(102) rocking curves were measured as shown in Fig. 4. The full-width-at-half-maximum of (002)/(102) rocking curve reflects screw and edge dislocation density. Sample A has the lowest dislocation density, with screw and edge dislocation densities in the order of 10^8 cm^2 and 10^9 cm^2, respectively. A LT AlN interlayer could deteriorate the crystal quality while the LT AlN interlayer with lower V/III ratio could invert the polarity of the subsequent GaN layer from N polarity to Ga polarity. Figure 5 shows the x-ray reciprocal-space-mapping (RSM) results of (002) plane of samples A–C. It can be seen that the insertion of LT AlN layer with different V/III ratio makes the (002) mapping broad along both q_{x-y} and q_z axis with different levels. Although LT AlN interlayer with high V/III ratio can inhibit the inversion of N-polarity, it leads to a large broadening in the q_{x-y} axis, implying serious tilt and short lateral coherence length.[11] The LT AlN interlayer with low V/III ratio not only broadens (002) mapping on the q_{x-y} axis but also broadens a lot on the q_z axis, which reflects the heterogeneity of the spacing between crystal planes in the *C*-axis direction.

Figure 6 shows the AFM results of three samples. Sample A had not only the best crystal quality but also the lowest surface roughness. The surface roughness of sample C was the highest, which was consistent with the analysis of the *in situ* reflectance results above. The polarity of sample B was inverted to Ga polarity, the surface bulge changed from sawtooth of N-polar GaN film to more rounded humps, which is related to the misorientation angle of the substrate. The surface of the inverted Ga-polar GaN film grown on the C-plane substrate without misorientation angle had reached the atomic level of roughness, as shown in our previous work.[9]

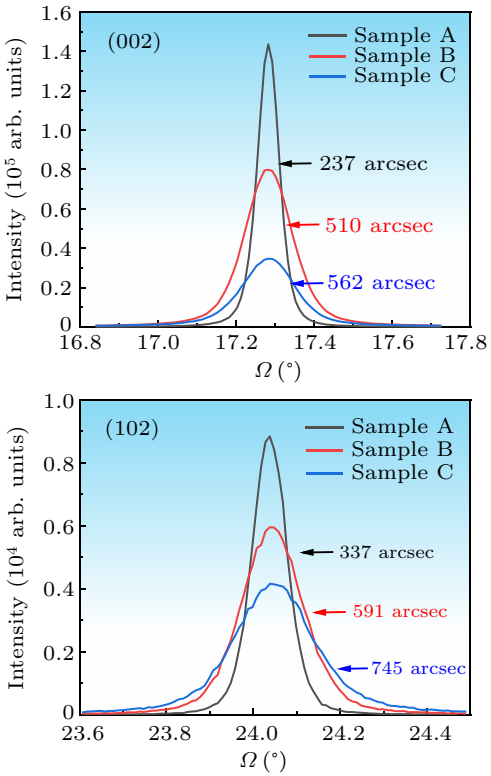


Fig. 4. The (002)/(102) x-ray rocking curve results of samples A–C.

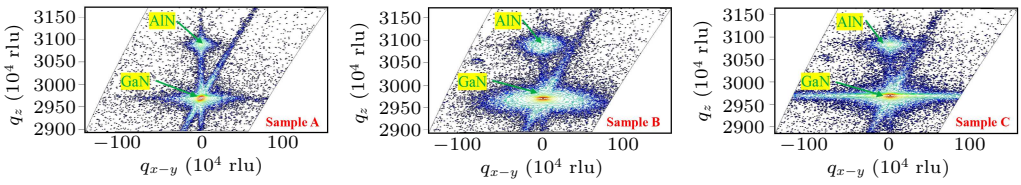


Fig. 5. X-ray RSM images of (002) plane of samples A–C.

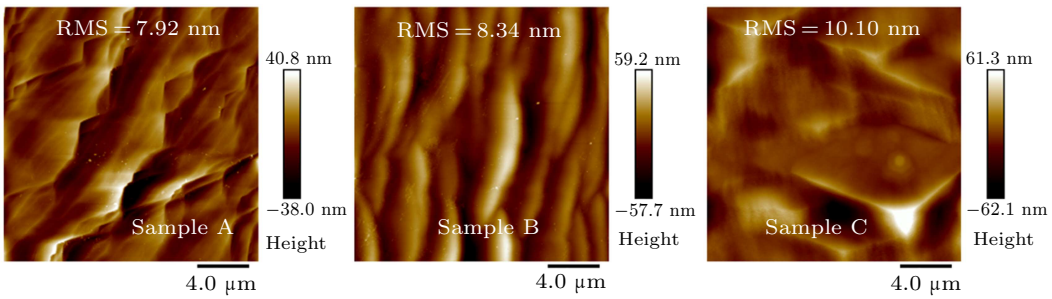


Fig. 6. AFM images (20×20 μm^2) of samples A–C.

To get more details of the AlN buffer layer, the growth was interrupted just before the GaN layer growth and the samples were measured by AFM, as shown in Fig. 7, and XPS, as shown in Fig. 8. After the growth of 100 nm HT AlN, many islands appeared on the surface of sample A, as shown in Figs. 7(a) and 7(d). These islands varied in size and were spaced widely from one island to another. The surface of sample C was also covered with many islands, as shown in Figs. 7(b) and 7(e). However, the islands of sample C were smaller, more uniform in size, and more densely distributed than those of sample A. At the beginning of GaN layer growth, these islands grew and began to coalesce, a lot of dislocations originated from the island coalescence boundary.[12] Therefore, smaller and denser islands will have more dislocations, explaining why sample C has more dislocation than sample A. It was interesting that no islands appeared on the surface of sample C, while its surface became very flat. As mentioned above, the polarity of sample B has been inverted to Ga polarity by a LT AlN interlayer with low V/III ratio. This phenomenon showed that the inversion occurred during the LT AlN growth because the atomic diffusion of Ga-polar surface was higher than that of N-polar surface, and thus formed a smoother surface. A previous article studied the effect of polarity on the morphology of LT GaN buffer layer.[13] Their results showed that the surface of N-polar LT GaN buffer layer was much rougher than that of Ga-polar buffer layer, which is consistent with our result.

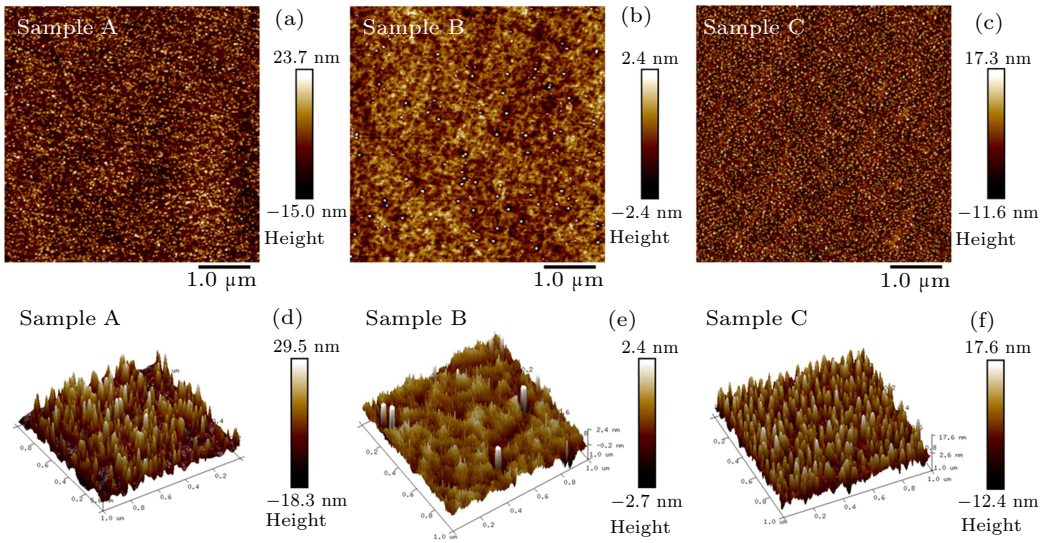


Fig. 7. The 2D (5×5 μm^2), 3D (1×1 μm^2) AFM images and statistical analysis of particle height of AlN buffer layers of (a), (d), (g) sample A; (b), (e), (h) sample B; and (c), (f), (i) sample C interrupted just before HT GaN layer growth.

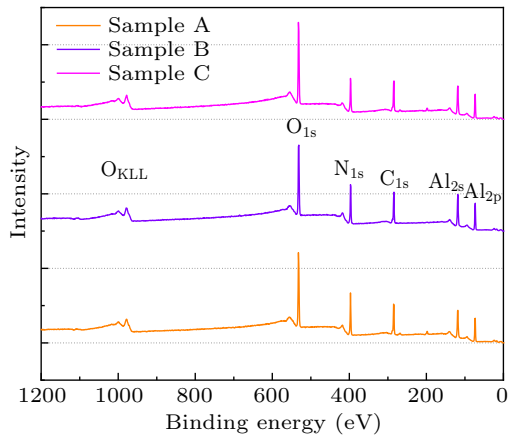


Fig. 8. XPS survey spectra of AlN buffer layers of samples A–C interrupted just before HT GaN layer growth.

Figure 8 shows the XPS survey scans of the AlN buffer layer of three samples and the spectra were calibrated to the C_{1s} peak at 284.8 eV.[14] The XPS spectra confirmed that these AlN buffer layers were mainly composed of aluminum, nitrogen, carbon, and oxygen elements. The carbon element was likely related to carbon-containing impurities originating from methyl of TMAl source or caused by adsorbed impurities. Due to the strong affinity between aluminum and oxygen elements, many oxygen elements were adsorbed on the surface of the AlN layer.

The atomic percentages of every element are shown in Table 1. It can be seen that the buffer layer of sample A was only a high-temperature AlN layer, and the atomic components of Al, N and O on the surface were 29.59%, 18.80%, and 26.22%, respectively. Compared with sample A, sample B had an extra layer of low-temperature AlN interlayer with the same growth conditions except temperature. With the decrease of temperature, the decomposition rate of NH_3 decreased rapidly, and the N atomic component on the surface of AlN decreased (17.37%). However, the O atomic component which competed to be incorporated into the lattice was increased (28.57%). For sample C, the V/III of low temperature AlN was continuously increased on the basis of lowering the temperature, it can be found that the N atomic component on

the surface of the AlN buffer layer was significantly increased (19.66%). Moreover, the O component was pressed down to 26.32% by the elevated N component. The higher composition of O atoms and the lower composition of N atoms promotes the formation of $Al_9O_3N_7$ structure, thus realizing the reversal of nitrogen polarity.[7]

Table 2. Atomic percentage of samples A–C.

Atomic (%)	Sample A	Sample B	Sample C
Al	29.59	30.01	30.53
N	18.80	17.37	19.66
O	26.22	28.57	26.32
C	25.40	24.05	23.49

4. Conclusion

The AlN buffer layer with high temperature and high V/III ratio can realize the epitaxial growth of high-quality N-polar GaN films. When the temperature decreases, the decomposition rate of NH_3 decreases rapidly, and the N/O element ratio drops sharply, resulting in more O atoms incorporated into the crystal lattice, thereby forming an $Al_3O_9N_7$ atomic structure that can lead to polarity inversion. Greatly increasing the V/III ratio can effectively increase the N/O element ratio in the reaction chamber, inhibiting the incorporation of O atoms into the crystal lattice, thereby maintaining the N polarity of the GaN film. In addition, the LT AlN interlayer would deteriorate the crystal quality and surface roughness of GaN films.

Data availability statement

The data that support the findings of this study are available from the corresponding author upon reasonable request.

Acknowledgements

Project supported by the National Natural Science Foundation of China (Grant No. 62004218) and the Strategic Priority Research Program of Chinese Academy of Sciences (Grant No. XDB33000000).

References

[1] Keller S, Li H R, Laurent M, *et al.* 2014 *Semicond. Sci. Technol.* **29** 113001
[2] Yen S H and Kuo Y K 2018 *J. Appl. Phys.* **103** 103115
[3] Keller S, Fichtenbaum N A, Furukawa M, Speck J S, DenBaars S P and Mishra U K 2007 *Appl. Phys. Lett.* **90** 191908
[4] Jennifer K H, Mark E T, Michael A M, Charles R E and Francis J K 2011 *Phys. Status. Solidi A* **208** 1504
[5] Wong M H, Wu F, Speck J S and Mishra U K 2010 *J. Appl. Phys.* **108** 123710
[6] Lim D H, Xu K, Arima S, Yoshikawa A and Takahashi K 2002 *J. Appl. Phys.* **91** 6461
[7] Stolyarchuk N, Markurt T, Courville A, March K, Zúñiga-Pérez J, Vennéguès P and Albrecht M 2018 *Scientific Reports* **8** 14111
[8] Su Z, Li Y, Hu X, Song Y, Kong R, Deng Z, Ma Z, Du C, Wang W, Jia H, Chen H and Jiang Y 2022 *Materials* **15** 3005
[9] Su Z L, Li Y F, Yin H B, Hai Y, Hu X T, Song Y M, Kong R, Deng Z, Ma Z G, Du C H, Wang W X, Jia H Q, Wang D H, Liu X Y, Jiang Y and Chen H 2022 *J. Cryst. Growth* **598** 126867
[10] Li Y F, Hu X T, Song Y M, Su Z L, Wang W Q, Jia H Q, Wang W X, Jiang Y and Chen H 2021 *Vacuum* **189** 110173
[11] Xu X Q, Li Y, Liu J M, Wei H Y, Liu X L, Yang S Y, Wang Z G and Wang H H 2013 *Appl. Phys. Lett.* **102** 132104
[12] Daniel D K, Michael E C, Stephen R L, Gerald Thaler, Karen C C and Michael J R 2008 *Proc. SPIE* **6841** 68410H
[13] Losurdo M, Giangregorio M M, Capezzuto P, Bruno G, Namkoong G, Alan Doolittle W and Brown A S 2004 *J. Appl. Phys.* **95** 8408
[14] Motamedi P and Cadien K 2014 *Applied Surface Science* **315** 104
[15] Rosenberger L, Baird R, McCullen E, Auner G and Shreve G 2008 *Surf. Interface Anal.* **40** 1254
[16] Sharma N, Ilango S, Dash S and Tyagi A K 2017 *Thin Solid Films* **636** 626